Heliyon 10 (2024) e38433

Contents lists available at ScienceDirect

Heliyon

journal homepage: www.cell.com/heliyon

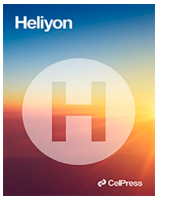

Research article

Hexadecylpyridinium bromides as a new capping agent for improving stability and luminescence of cesium lead bromide perovskites

Christina Al Tawil, Riham El Kurdi, Digambara Patra *

Department of Chemistry, American University of Beirut, Beirut, Lebanon

ARTICLE INFO

Keywords:
$CsPbBr_3$
CTAB
CPB
PLQY
PbI_2
Anion exchange
Stabilization
Crystal structure

ABSTRACT

Because of exception properties, inorganic halide perovskites are promising materials for numerous applications. The efficiency of these materials are evaluated based on their photoluminescence quantum yield, which is the key indicator and proportional to the stability of the perovskite. Hence, to limit the instability of the perovskites, addition of surfactant as ligand has been applied during synthesis of nanoparticle based inorganic perovskite $CsPbBr_3$. As far as we know, only a few researchers have studied the impact of hexadecylpyridinium bromide (CPB) on the stability of the crystal structure of $CsPbBr_3$. In this work, we present a novel approach for lead halide perovskites by incorporating CPB to primarily maintain the perovskite's crystal structure, and later on to enhance the stability of $CsPbBr_3$ NPs while boosting its photoluminescence quantum yield (PLQY). Results showed that CPB enhanced the thermal stability and boosted the PLQY to 90 %. Moreover, CPB had proven its efficiency as a capping agent preventing the exchange of anion between bromide and iodide ions in presence of lead iodide.

1. Introduction

Surface defects highly influence the electronic and optical properties of lead halide perovskites [1]. In fact, the atomic composition of perovskite crystals can differ between their interior and exterior surfaces. This leads to the formation of unwanted quantum states within the energy band gap, which adversely impacts the optoelectronic properties and reduces photoluminescence (PL) stability [2]. The straightforward solution-based fabrication of perovskite thin films [3] often leads to uncontrollable defects, such as uncoordinated Pb^{2+} and halide vacancies, which create non-radiative recombination sites and reduce the photoluminescence quantum yield (PLQY) of the perovskite [4]. A recent review documented by Konidakis et al. shows the importance of composite glasses with metallic perovskite, for the optoelectronic and photonic applications [5]. Growing research on the incorporation of stabilizing surfactants into perovskites has demonstrated improvements in quantum yield [5,6]. Notably, enhancing surface passivation with salt solutions [7], introducing alternative cation/anion compositions through doping [8], or employing post-synthetic ion exchange [9] are regarded as the most effective methods for boosting the PLQY of perovskites.

Many researchers investigated chemical passivation techniques to reduce defect formation and address this issue [10]. Surface ligand exchange in perovskites has been shown to stabilize the material and improve its PLQY [11].

Indeed, CPB is a pyridinium salt that, once dissolved in a solution, is made up of an organic cation N-hexadecyl pyridinium and a

* Corresponding author.
E-mail address: dp03@aub.edu.lb (D. Patra).

https://doi.org/10.1016/j.heliyon.2024.e38433
Received 31 May 2024; Received in revised form 23 September 2024; Accepted 24 September 2024
Available online 25 September 2024

bromide anion. Its functional groups are amines and heterocycles [12]. The cation exhibits a a positively charged pyridinium ring that acts as a polar head, along with a long aliphatic cetyl chain serving as the nonpolar tail [13]. The difference between CPB and CTAB cations is only found in the positively charged ionic head structure, while hydrophobic alkyl chain is same for both (See Scheme 1). CPB has a pyridine while CTAB has a trimethylamine head structure. Amines react with the surface of perovskites, CPB and CTAB act as nucleophiles. The nucleophilicity of amines increases with basicity but is affected by steric hindrance. In trimethylamine (more sterically hindered), the N atom is sp^3 hybridized while in pyridine the N atom is sp^2 hybridized. sp is more reactive than sp^2, and sp^2 is more reactive than sp^3. Thus CPB is a better ligand. This difference in the chemical structure made CPB adsorb chemically while CTAB adsorb physically [14]. In fact, the increased efficiency of CPB over CTAB is due to the charge on the nitrogen atom [15].

In our work, to regulate the synthesis of inorganic cesium lead halide perovskite nanoparticles, hexadecylpyridinium bromide was used for the first time in the formation of $CsPbX_3$ perovskites using the hot injection method with surfactant ligand. Subsequently, CPB was doped to preserve crystal structure of $CsPbBr_3$ and maintain its strong green photoluminescence (PL) emission. Results show enhancement in PLQY and imrpoved stability of the prepared $CsPbX_3$ perovskites till 90 %. Moreover, CPB prevents the anion exchange between bromide and iodide ions upon the addition of PbI_2 to the perovskite.

2. Materials and methods

2.1. Materials

Acros Organics supplied Hexadecyltrimethyl-ammonium bromide (CTAB, $C_{19}H_{42}BrN$, 99 %), Cesium Carbonate (Cs_2CO_3, 99.5 %), Hexadecylpyridinium bromide (CPB, $C_{21}H_{38}BrN$, 98 %), 1-Octadecene (ODE, $C_{18}H_{36}$, 90 %), Lead (II) iodide (PbI_2, 99 %), Oleylamine (OAm, $C_{18}H_{37}N$, 80–90 %), and Sulphuric acid (H_2SO_4, 32 %) were obtained. Fisher Scientific Company supplied lead (II) bromide ($PbBr_2$, 99 %). Sigma Aldrich supplied Oleic acid (OA, $C_{18}H_{34}O_2$, 65–88 %) and hexane (C_6H_{14}, 97 %). Fluka Analytical supplied Quinine anhydrous ($C_{20}H_{24}N_2O_2$, 98 %). Without purifying further all chemicals were used.

2.2. Cesium oleate solution synthesis

First, a stock solution containing 0.053 M of cesium carbonate (m = 0.4 g) was made with oleic acid (1.24 mL) and octadecene (20 mL). At 200 °C, solutions were continuously stirred. A visible change in color from transparent to yellowish confirmed the complete dissolution of Cs_2CO_3 and, consequently, cesium oleate was prepared. In order to preserve it for later use, the solution of cesium oleate was vacuum packed and stored at room temperature.

2.3. Synthesis of CPB-oleate solution and CTAB-oleate solution

0.050 g of CTAB (C = 0.013 mol/L) in 10 mL ODE was mixed with 0.62 mL OA to prepare CTAB-oleate, similarly 0.053 g of CPB (C = 0.013 mol/L) in 10 mL ODE was mixed with 0.62 mL OA to make CPB-oleate solution. In both cases the color changed from translucent to yellow after stirring and heating at 200 °C, revealing reactants' complete dissolution. For later usage, the resulting solutions were packaged and stored at room temperature. It should be noted that low concentrations of both CPB and CTAB didn't lead to the formation of perovskites whereas the excess of the surfactant at high concentrations of CPB and CTAB decreased the physical properties such as crystallinity, fluorescence of the formed perovskites.

2.4. Lead bromide perovskites synthesis

Firstly, $PbBr_2$ (0.08 g, C = 0.0363 M) was mixed with ODE (5 mL) in an airless atmosphere at 190–200 °C for 10 min. Then OA (0.5 mL) was added followed by OAm (0.5 mL) and stirred till all $PbBr_2$ is dissolved. The reaction mixture was then quenched by submerging it in a 10 °C cold water bath, afterwards Cs-oleate (0.4 mL) was introduced. After centrifuging at 15000 rpm for 15 min, the precipitate was collected and employed for additional characterization after being dissolved in 5 mL of hexane.

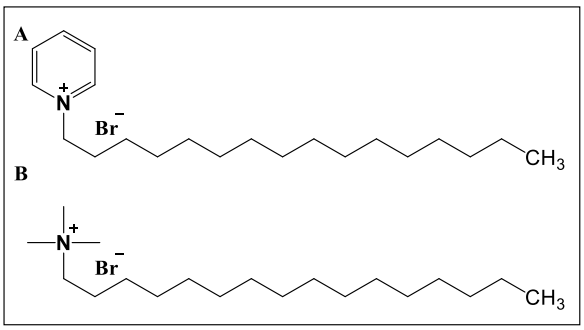

Scheme 1. Chemical structure of (A) hexadecylpyridinium bromide CPB; and (B) Hexadecyltrimethyl ammonium bromide CTAB.

2.5. Enhancement of the perovskites stability

The stability of the material is critical in terms of its efficiency. For this purpose, the addition of a stabilizing agent of either CPB or CTAB was tested. $PbBr_2$ was prepared as previously described, followed by the addition of 2 mL of either CPB-oleate or CTAB-oleate and cesium oleate solution (1.2 mL). After the reaction was completed, the solutions were immersed in a cold bath, centrifuged, and the resulting precipitate was dissolved in hexane.

2.6. Sample preparation for PLQY measurement

As an initial step, 1 mM solution of quinine solution was prepared in 0.5 M H_2SO_4 solution. For PLQY measurement values, fluorescence spectra were recorded for the $CsPbBr_3$ and quinine solution as reference.

2.7. Effect of PbI_2 on the stability of $CsPbBr_3$

Initially, 10 μL of the prepared peovskites either with CPB-oleate or with CTAB-oleate solution were pipetted, placed on a glass slide, and then to eliminate hexane it was kept overnight at 30 °*C* in a vacuum oven. Henceforth, the slide was immerged in a 3 mL cuvette and placed in the holder of the fluorometer. The emission spectra were measured while gradually increasing the concentration of PbI_2 (from 0.0072 μM to 0.024 μM). For this, PbI_2 solution (0.043 μM) was made in double distilled water (10 mL), and the needed volumes were pipetted.

2.8. Spectroscopic analysis and characterization

The primary method used to determine the optical characteristics of the produced perovskites was fluorescence emission spectroscopy. For this a Jobin-Yvon-Horiba Fluorolog III fluorometer accompanying a FluorEssence software were utilized. As a excitation source, a Xenon lamp (100 W) was used and a R-928 detector was applied to collect the emission, and the slit widths were maintained at 5 nm. To measure ultraviolet–visible (UV–vis) absorption spectra JASCO V-570 UV–VIS–NIR spectrophotometer was utilized. In these measurements, total volume was kept 3 mL by pipetting 0.2 mL of $CsPbBr_3$ perovskites and diluting with hexane. For exterior morphological characterization, SEM (Scanning Electron Microscopy) was applied attached with a Tescan, Vega 3 LMU with Oxford EDX detector (Inca XmaW20). For understanding thermal stability a Netzsch TGA 209 instrument was used for TGA (Thermogravimetric analysis) in 30–900 °C temperature range, with a 15 °C/min increment in a N_2 environment. For measurement, few microlitre of $CsPbBr_3$ solution was filled in an aluminum oxide crucible and heated to 45 °C until complete evaporation of hexane. Afterwards this crucible was placed in the holder of TGA machine. The steady mass the crucible had after 30 min served as evidence of the complete evaporation of hexane.

3. Results and discussion

3.1. Characterization of $CsPbBr_3$ perovskites prepared in the presence of CPB and CTAB

The UV–visible absorption and fluorescence spectra of $CsPbBr_3$ perovskites prepared with different capping agents, CTAB and CPB, were assessed to examine the optical properties. The doped $CsPbBr_3$ perovskites, as shown in Fig. 1A, did not display a remarkable shift in the absorption wavelength maximum ($\lambda_{abs} = 475$ nm) and emission wavelength maximum ($\lambda_{em} = 510$ nm) confirming that capping agent did not alter the initial $CsPbBr_3$ crystal structure. However, there were changes in absorbance and photoluminescence intensity. Absorbance values were the only difference between CPB and CTAB doped $CsPbBr_3$. CPB doped $CsPbBr_3$ gave the maximum

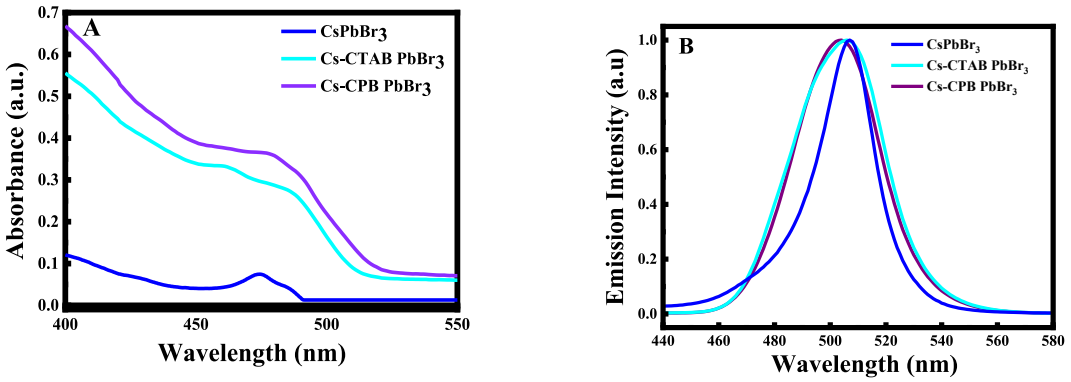

Fig. 1. $CsPbBr_3$ perovskites prepared using CPB (Cs-CPB $PbBr_3$) and CTAB (Cs-CTAB $PbBr_3$) as capping agents. (A) UV–Visible absorption spectra and (B) Normalized fluorescence emission spectra.

absorbance ($A_{CPB} = 0.364$a.u > $A_{CTAB} = 0.283$a.u) indicating in this case formation of $CsPbBr_3$ is more which encourages materialization yield.

Additionally, the successful synthesis of perovskites was confirmed through fluorescence emission spectra, as shown in Fig. 1B. Interestingly, the addition of either CPB or CTAB to the lead bromide perovskite exhibited remarkable enhancement in photoluminescence intensity around ~1.74 fold in the presence of CPB and ~1.43 in the presence of CTAB, at λ_{em} = 500–506 nm. This enhancement in photoluminescence intensity at this particular (same) wavelength suggests an increase in radiative recombination. And this increment can be because of association of bromide anions, cetylpyridinium cations and cetyltrimethylammonium cations to surface defects on the lead bromide perovskite crystals, which decreases non-radiative recombination centers, like uncoordinated Pb cations and halide vacancies [16]. However, a very small blue shift is obtained when CPB was added from 507 nm to 502 nm. Thus, the shift towards shorter wavelength in the fluorescence emission wavelength maximum is linked to the size of the NPs. For instance, as the emission wavelength maximum shifts to blue (shorter wavelength), smaller and more uniform NPs are formed. SEM imgaes further established this fact. Notable distinctions were found in crystal morphology between $CsPbBr_3$, Cs-CTAB $PbBr_3$, and Cs-CPB $PbBr_3$. When CPB is added, smaller CsPbBr3 nanoparticles were obtained, which can be concluded from the sharp peak shapes found in the emission spectra as depicted in Fig. 2A–C.

The scattering observed in the absorbance spectra is due to the polydisperse sample shown in the SEM images of $CsPbBr_3$ and Cs-CTAB $PbBr_3$ (Fig. 2 A and C), which broadens the full width at half maximum (Fig. 1b). However, comparing CPB and CTAB, the sharper peak obtained in the fluorescence emission of Cs-CPB $PbBr_3$ is due to the better monodispersity of these particles as confirmed by the small and uniform nanoparticles in Fig. 2B (compared to Fig. 2C). XRD patterns given in Fig. 2D also confirms formation of $CsPbBr_3$ nanocrystals.

Additionally, a band tail is observed in the PL emission of Cs-CTAB $PbBr_3$ and absent in Cs-CPB $PbBr_3$. Typically band tail states are considered nonradiative traps for photocarriers. Given the small particle size, with most atoms being surface atoms, these tail states are likely originating from the surface region, possibly induced by ligands. Exchanging ligands could significantly reduce PL tail. This confirms that CPB is a better ligand in passivating defects and therefore reducing traps, which is also proved by the significant improvement in PL intensity in the presence of CPB compared to CTAB.

The synthesized $CsPbBr_3$ perovskites gave many diffraction peaks at 2θ values of 12.73°, 15.22°, 25.55°, and 30.74°, these results confirm the formation of 3D structure perovskites. All the prepared **$CsPbBr_3$** perovskites results were similar when doped with CPB or CTAB.

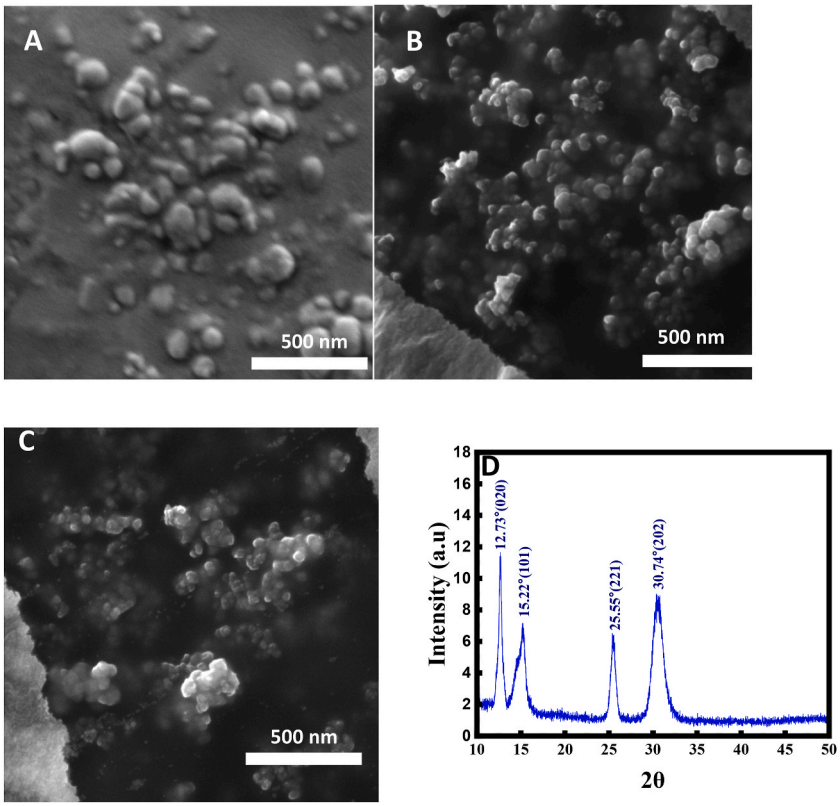

Fig. 2. SEM images of $CsPbBr_3$ perovskites (A) in the presence of cesium oleate only ($CsPbBr_3$); (B) in the presence of cesium oleate and CPB (Cs-CPB$PbBr_3$); (C) in the presence of cesium oleate and CTAB (Cs-CTAB$PbBr_3$); and (D) XRD pattern of $CsPbBr_3$.

3.2. TGA of $CsPbBr_3$ doped with either CPB or CTAB

As depicted in Fig. 3A, thermogravimetric analysis was performed to evaluate the thermal stability of the prepared $CsPbBr_3$ nanoparticles doped with either CPB or CTAB. The analysis revealed a unique profile marked by three distinct thermal events, as indicated by the corresponding weight percent derivative given in Fig. 3B.

In the lower temperature between 25 $°C-$ 200$°C$, a slight mass loss of around 10 % was observed for both $CsPbBr_3$ doped with either CPB or CTAB. This loss in weight is attributed to oleic acid evaporation and the removal of surface ligands from capped alkyl amines, as documented in the literature [17,18]. Boote et al. noted that because of the presence of oleylamine and oleic acid ligands, lead halide perovskites lose the majority of their mass in this temperature range. At higher temperatures between 200 $°C-$ 400$°C$, the additional weight loss can be attributed to the sublimation of Hexadecyltrimethyl ammonium bromide (CTAB). According to Grisorio et al. instead of decomposition of the perovskite, sublimation of ammonium halides causes this weight loss at this range [17,18].

The thermal decomposition (>480 °C) can be due to decomposition of inorganic core following sublimation of their original constituents ($PbBr_2$ and CsBr). This degradation pattern was identical to TGA results obtained by Xu et al. As proved in the literature, the weight loss of 15 % that occurs in 375–480 °C temperature range of was proved to be due to $PbBr_2$ sublimation of at a very high temperatures [19,20].

This loss was huge in OA/OLA $CsPbBr_3$ compared with Cs-CPB $PbBr_3$ nanoparticles. The variation in the degradation patterns of the two components indicates that $PbBr_2$ within the perovskite undergoes less degradation, suggesting it is more stable. Therefore, doping of CPB or CTAB reduces $CsPbBr_3$ perovskite's decomposition and degradation. Hence, the enhancement of the thermal stability of Cs-CPB $PbBr_3$ compared with OA/OLA $CsPbBr_3$ is due to the stronger binding of CPB to the surface of nanoparticles through the pyridine ionic head which passivates the Pb^{2+} and Br^- defects on the surface of the nanoparticles and acts as a strong capping ligand.

3.3. PLQY of $CsPbBr_3$ doped with either CPB or CTAB

PLQY measurement is considered as an essential parameter of the luminescent material. Consequently, PLQY was measured and the effect of CTAB and CPB on $CsPbBr_3$'s photoluminescence was studied by comparing with PLQY percentage values. PLQY was estimated by using quinine sulfate dihydrate as a reference fluorophore, whose standard quantum yield is 0.546 in 400–600 nm emission wavelength range. According to Nawara et al. up to 45 °C, quinine has no temperature sensitivity, making it a trustworthy as a reference solution for the PLQY measurements [5]. The synthesized $CsPbBr_3$ were analyzed by fluorescence emission intensity.

Fascinatingly, while comparing percentage of PLQY (% PLQY) value, it was found that % PLQY of $CsPbBr_3$ extraordinarily increased to ~90 % when CPB was doped (Cs-CPB$PbBr_3$) in contrast to 75 % improvement when doped with CTAB (Cs-CTAB$PbBr_3$) and 17 % in the absence of any surfactant, as compared in Fig. 4. This extraordinary increase is caused by passivation of defects of Pb^{2+} and Br^- ion introduced by CPB, as this can be caused by the pyridinium groups present in CPB. Indeed, CPB has a dual function as a capping agent and doping of crystal. CPB salt is dissociated into bromide ions and organic cation. With the first addition, either bromide ions are incorporated into the crystal, or the cation is replacing cesium atom. As for the second addition, CPB acts as a capping agent to stabilize the crystal. The comparision of percentage of PLQY (PLQY %) values obtained in the present study with that from the literature is summarized in Table 1.

3.4. Variation in the photoluminescence of $CsPbBr_3$ upon the addition of PbI_2 in the presence of either CPB or CTAB

In the presence of either CPB or CTAB the photoluminescence spectra were recorded to access the effect of lead iodide (PbI_2).

According to Fig. 5, in both cases, initially the photoluminescence wavelength maximum was found to be around 500 nm. This confirms successful synthesis of $CsPbBr_3$ perovskites. However, when adding water, the photoluminescence intensity of $CsPbBr_3$ in the presence of CTAB decreased as shown in Fig. 5A. This essentially is due to dissociation of the $CsPbBr_3$ perovskite crystal into its ions

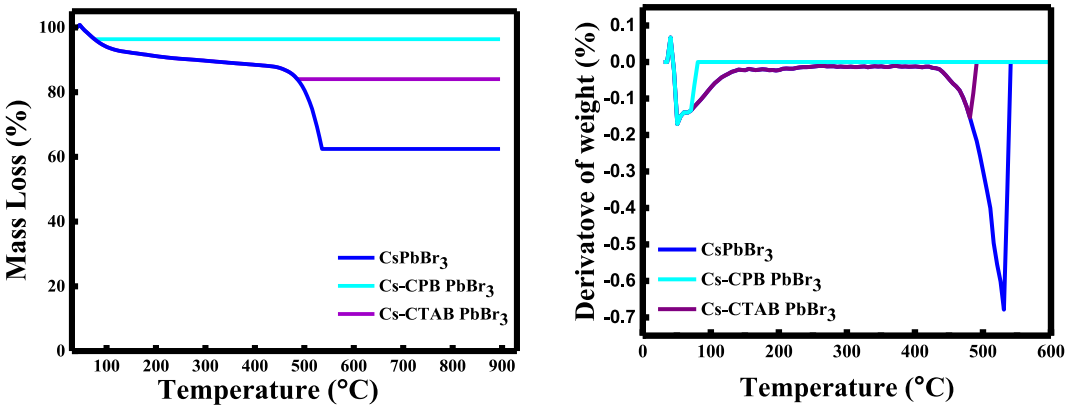

Fig. 3. (A) TGA (thermogravimetric analysis) of lead bromide perovskites; (B) Corresponding first derivative of TGA.

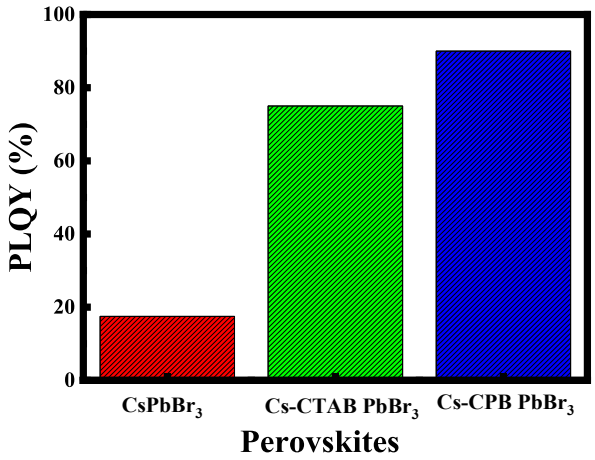

Fig. 4. PLQY of $CsPbBr_3$ perovskites and its comparision in the presence of CPB (Cs-CPB$PbBr_3$) and CTAB (Cs-CTAB$PbBr_3$).

Table 1
Comparision of percentage of PLQY (PLQY %) values obtained in the present study with that from the literature.

Perovskites	PLQY %	References
methylammonium lead bromide/formate mixture	69	[21]
$CsPbBr_3$ Nanocrystal Solid-State Films	54	[22]
$CsPbBr_3$ doped with $ZnBr_2$-CPB	30	[23]
CPB doped $CsPbBr_3$ perovskites	99	Our work

due to the presence of water. Remarkably, a shift to longer wavelength (red shift) from 506 nm to 520 nm and a continuous quenching in the photoluminescence intensity were obtained when adding PbI_2 to $CsPbBr_3$ perovskites. This shift in maximum and decrease in intensity confirm exchange of anion between Br^- ion and I^- ion inducing the formation of $CsPb[Br/I]_3$ perovskites.

However, in the presence of CPB, it is obvious that when adding water, the emission intensity remains constant (See Fig. 5B). Thereby, in the presence of CPB, the lead bromide inside the perovskites was not affected and therefore protected from any other interactions. Henceforward, when adding PbI_2 solution, from (0.2 mL–0.8 mL), the emission intensity slightly decreases with no remarkable shift. Hence, this is due to the fact that PbI_2 molecules are being attracted to the pyridinium group present in CPB molecules, inducing the formation of CPB-PbI_3 perovskites. Thus, at higher volume of PbI_2 (1 mL and 1.2 mL) a significant shift from 509 nm to longer wavelength, 520 nm, was obtained, inducing therefore the penetration of PbI_2 into the perovskites and therefore the formation of Cs-CPB-$[Br/I]_3$ perovskites. This finding confirms the function of capping agent, CPB, in preserving the crystal structure of $CsPbBr_3$. In fact, the difference in the photoluminescence response is related to the CPB and CTAB as capping agents or ligands, their contact with the surface/interface of the nanocrystals, and how easily they can detach from the surface of NCs exposing the NCs to water. Although, CPB has a pyridine ring with Br^- anion, while CTAB has a quaternary nitrogen (N^+) atom with a cetyl chain. CPB with pyridine rings causes stronger intermolecular force due to $\prod$-conjugation (p-conjugation) which means stronger interaction with surface of nanocrystals. CPB and CTAB have hydrophobic covalent bonding forces in their alkyl chain which decreases their surface tension and makes them a good cationic surfactant instead of emulsifying with water. CPB has lower surface tension than CTAB due to the pyridine ring so it's a better surfactant with higher hydrophobic interactions. Also, the density of CPB is 1.2 g/cm^3 compared with CTAB 0.5 g/cmˆ3, which means that when water is added (density 1 g/cm^3), less interactions occur with CPB [24].

4. Conclusion

In conclusion, $CsPbBr_3$ was successfully made using a straightforward hot-injection method. It further was verified that CPB outperformed CTAB as a stabilizing agent, owing to the binding of cetylpyridinium and bromide ions to surface defects on the $CsPbBr_3$ nanocrystals. Moreover, the produced nano-perovskites were found to be spherical at a scale bar of 500 nm. Furthermore, the presence of CPB causes improvement in $CsPbBr_3$'s thermal stability because of the presence of pyridinium groups respectively that enhance the incorporation of $PbBr_2$ inside the perovskites. Henceforth, doping of CPB increased PLQY value to 90 %. Conclusively, CPB acts as a capping agent in preserving $CsPbBr_3$'s crystal structure and preventing exchange of anion between Br^- ion and I^- ion upon the addition of low concentrations of PbI_2.

Data and code availability

The authors are unable or have chosen not to specify which data has been used.

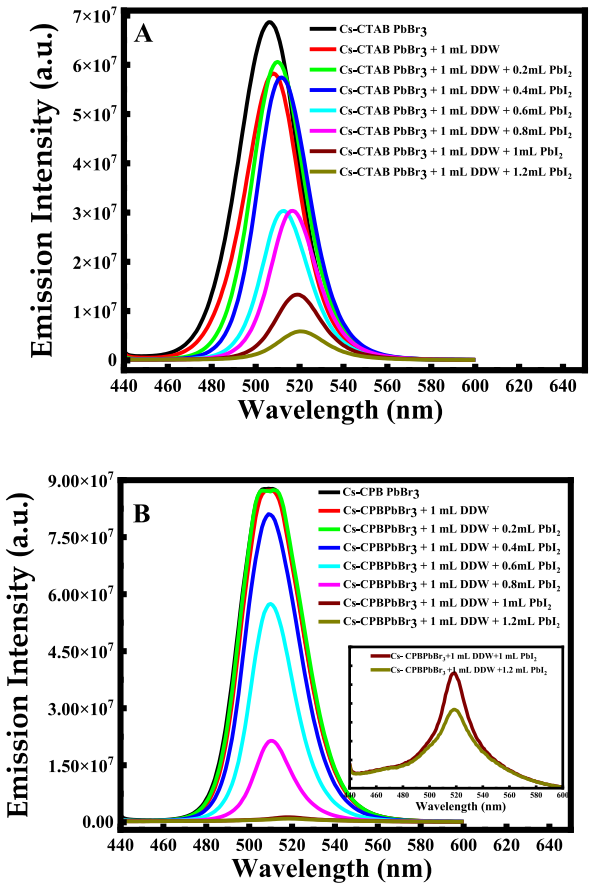

Fig. 5. Variation of the fluorescence emission intensity of $CsPbBr_3$ upon the addition of PbI_2 (A) doping with CTAB and (B) doping with CPB. The inset in Fig. 5B shows the variation of the emission spectra in the presence of 1 mL and 1.2 mL of PbI_2.

CRediT authorship contribution statement

Christina Al Tawil: Writing – review & editing, Methodology, Formal analysis, Data curation. **Riham El Kurdi:** Writing – review & editing, Validation, Project administration, Investigation, Data curation. **Digambara Patra:** Writing – review & editing, Project administration, Conceptualization.

Declaration of competing interest

The authors declare that they have no known competing financial interests or personal relationships that could have appeared to influence the work reported in this paper.

Acknowledgements

Kamal A. Shair Central Research Laboratory (KAS CRSL) facilities at American University of Beirut (AUB), Lebanon and financial support by University Research Board (URB) of AUB are acknowledged.

References

[1] K.J. Savill, A.M. Ulatowski, L.M. Herz, Optoelectronic properties of tin-lead halide perovskites, ACS Energy Lett. 6 (7) (2021) 2413–2426.
[2] S. Lee, D. B. Yu Kim, J.C. Jang, H. C, J.H. Park, B.R. Lee, M.H. Song, Versatile defect passivation methods for metal halide perovskite materials and their application to light-emitting devices, Adv. Mater. 31 (20) (2019) 1–17.
[3] Li, M.H. Yeh, H.-H. Chiang, Y.-H. Jeng, U.-S. Su, C.-J. Shiu, H.-W. Hsu, Y.-J. Kosugi, N. Ohigashi, T. Chen, Y.-A. Shen, P.-S. Chen, P. Guo, T-G. Highly efficient 2D/3D hybrid perovskite solar cells via low-pressure vapor-assisted solution process, Adv. Mater. 30 (30) (2018) 1–13.
[4] G. Ahmed, J. Yin, O.M. Bakr, O.F. Mohammed, Near-unity photoluminescence quantum yield in inorganic perovskite nanocrystals by metal-ion doping, J, Chem. Phys. 152 (2) (2019) 020902.
[5] I. Konidakis, A. Karagiannaki, E. Stratakis, Advanced composite glasses with metallic, perovskite, and two-dimensional nanocrystals for optoelectronic and photonic applications, Nanoscale 14 (8) (2022) 2966–2989.

[6] F. Liu, Y. Zhang, C. Ding, S. Kobayashi, T. Izuishi, N. Nakazawa, T. Toyoda, T. Ohta, S. Hayase, T. Minemoto, K. Yoshino, S. Dai, Q. Shen, Highly luminescent phase-stable CsPbI3 perovskite quantum dots achieving near 100% absolute photoluminescence quantum yield, ACS Nano 11 (10) (2017) 10373–10383.
[7] Wang, S. Wang, Y. Zhang, Y. Zhang, X. Shen, X. Zhuang, X. Lu, P. Yu, W.W. Kershaw, S.V. Rogach, A.L. Cesium, Lead chloride/bromide perovskite quantum dots with strong blue emission realized via a nitrate-induced selective surface defect elimination process 10 (1) (2019) 90–96.
[8] M. Lu, X. Zhang, X. Bai, H. Wu, Spontaneous silver doping and surface passivation of CsPbI3 perovskite active layer enable light-emitting devices with an external quantum efficiency of 11.2, ACS Energy Lett. 3 (7) (2018) 1571–1577.
[9] S.F. Solari, S. Kumar, J. Jagielski, N.M. Kubo, F. Krumeich, C.J. Shih, Ligand-Assisted solid phase synthesis of mixed-halide perovskite nanocrystals for color-pure and efficient electroluminescence, J. Mater. Chem. C 9 (17) (2021) 5771–5778.
[10] H. Zhang, Y. Wu, C. Shen, E. Li, C. Yan, W. Zhang, H. Tian, L. Han, W.-H. Zhu, Efficient and stable chemical passivation on perovskite surface via bidentate anchoring, Adv. Energy Mater. 9 (13) (2019) 1–9.
[11] L.M. Wheeler, E.M. Sanehira, A.R. Marshall, P. Schulz, M. Suri, N.C. Anderson, J.A. Christians, D. Nordlund, D. Sokaras, T. Kroll, S.P. Harvey, J.J. Berry, L.Y. Lin, J.M. Luther, Targeted ligand-exchange chemistry on cesium lead halide perovskite quantum dots for high-efficiency photovoltaics, J. Am. Chem. Soc. 140 (33) (2018) 10504–10513.
[12] R. Verma, A. Mishra, K.R. Mitchell-Koch, Molecular modeling of cetylpyridinium bromide, a cationic surfactant, in solutions and micelle, J. Chem. Theory Comput. 11 (1) (2015) 5415–5425.
[13] M. Fizer, O. Fizer, Theoretical study on charge distribution in cetylpyridinium cationic surfactant, J. Mol. Model. 27 (7) (2021) 203.
[14] M.M. Saleh, A.A. Atia, Effects of structure of the ionic head of cationic surfactant on its inhibition of acid corrosion of mild steel, J. Appl. Electrochem. 36 (8) (2006) 899–905.
[15] S.A.A. El-Maksoud, The effect of hexadecyl pyridinium bromide and hexadecyl trimethyl ammonium bromide on the behaviour of iron and copper in acidic solutions, J. Electroanal. Chem. 565 (2) (2004) 321–328.
[16] K. Srisawad, P. Kanjanaboos, P. Wilairat, S. Sahasithiwat, P. Pakawatpanurut, Enhanced electroluminescence of cesium lead bromide light-emitting diode driven by ion migration via surface passivation with organic halide surfactants, Surf. Interf. 30 (2022) 101853.
[17] R. Grisorio, C.N. Dibenedetto, A. Matuhina, G.A. Gandhi, P. Vivo, E. Fanizza, M. Striccoli, G.P. Suranna, Synthetic control over the surface chemistry of blue-emitting perovskite nanocrystals for photocatalysis, ACS Appl. Nano Mater. 6 (9) (2023) 8082–8092.
[18] B.W. Boote, H.P. Andaraarachchi, B.A. Rosale, R. Blome-Fernandez, F. Zhu, M. Reichert, K. Santra, J. Li, J.W. Petrich, J. Vela, E.A. Smith, Unveiling the photo- and thermal-stability of cesium lead halide perovskite nanocrystals, ChemPhysChem 20 (20) (2019) 2647–2656.
[19] P. Acharyya, P. Pal, P.K. Samanta, A. Sarkar, S.K. Pati, K. Biswas, Single pot synthesis of indirect band gap 2D CsPb2Br5 nanosheets from direct band gap 3D CsPbBr3 nanocrystals and the origin of their luminescence properties, Nanoscale 11 (9) (2019) 4025–4034.
[20] T. Xu, L. Chen, Z. Guo, T. Ma, Strategic improvement of the long-term stability of perovskite materials and perovskite solar cells, Phys. Chem. Chem. Phys. 18 (39) (2016) 27026–27050.
[21] Y. Khan, Y. Ahn, H. Lee, J. Jeong, Y.S. Shin, J.S. Lee, J.H. Kwon, J.Y. Kim, H.S. Kim, J.H. Seo, B. Walker, Waterproof perovskites: high fluorescence quantum yield and stability from a methylammonium lead bromide/formate mixture in water, J. Mater. Chem. C 8 (17) (2020) 5873–5881.
[22] F. Di Stasio, S. Christodoulou, N. Huo, G. Konstantatos, Near-Unity photoluminescence quantum yield in CsPbBr3 nanocrystal solid-state films via postsynthesis treatment with lead bromide, Chem. Mater. 29 (18) (2017) 7663–7667.
[23] J. Park, Y. Kim, S. Ham, J.Y. Woo, T. Kim, S. Jeong, D. Kim, A relationship between the surface composition and spectroscopic properties of cesium lead bromide (CsPbBr3) perovskite nanocrystals: focusing on photoluminescence efficiency, Nanoscale 12 (3) (2020) 1563–1570.
[24] M. Singh, N. Chaudhary, R.K. Kale, H.S. Verma, Molecular interactions of CPC, CPB, CTAB, and EPC biosurfactants in aqueous olive oil mixtures analyzed with physicochemical data and SEM micrographs, Arab. J. Chem. 7 (6) (2014) 1039–1048.